Modeling and Simulations of Multi-Dimensional Thermal Behaviors of Plates During Friction Stir Additive Manufacturing

Olurotimi Adeleye [a,*], Gbeminiyi Sobamowo [b]

[a] *Biomedical Engineering Dept., University of Lagos, Akoka, Lagos, +234, Nigeria*
[b] *Mechanical Engineering Dept., University of Lagos, Akoka, Lagos, +234, Nigeria*

Abstract

Friction-stir additive manufacturing is a type of solid-state additive manufacturing process that involves intense shear deformation of material during the material joining process. The increasing application of the novel technology requires proper understanding of the inherent thermal process. The analysis of the transient thermal behavior in three dimensions of the welded plates in friction-stir additive manufacturing is studied using Laplace transforms method is presented. It was established from the results that the material reduces in temperature during the simulation process as the distance of the point moving heat source increases from the centerline. Also, the time needed to attain the highest temperature increases with increasing distance between the point moving heat source and the centerline. In addition, the heating and cooling rates decrease while the distance between the point moving heat source and the centerline increases. The peak temperature is approximately 1200oC but this depends on the welding conditions, heat generation the materials, etc. The variation of shoulder heat generation rate with welding rotational speed at different welding velocities of 100-200 mm/min depicts that increasing the tool rotational speed at constant weld speed increases the heat input, whereas the heat input decreases with an increase in the weld speed at constant tool rotational speed. It was also established that the fractional heat generation rate is between 80 to 90% heat is generated at the tool shoulder and the remaining amount at other tool surfaces. However, this depends on the welding conditions. Finally, the temperature profile typical features can be observed from the obtained results at varying monitoring points, and they provide a better analysis of the prevailing factors in the heat flow model for a point moving heat source. Hence, the model and analytical solution provide the benchmark for obtaining temperature profiles for point moving heat source during the additive manufacturing process.

Keywords: Thermal analysis; Three-dimensional model; Frictional Stir Manufacturing; Analytical solutions**.**

---

* Corresponding author. Tel.: +2348055225840
E-mail address: rotimiadeleye1711@gmail.com

1. Introduction

Additive manufacturing (AM) has been one of the most widely used techniques in the area of zero waste manufacturing. Being able to manufacture any part within the stipulated time and with almost negligible down time, AM has touched the level of extreme manufactured techniques. Since the introduction of AM, manufacturing at various levels, such as macro to micro, has been achieved. With the introduction of nanomanufacturing and by using nanomaterials, AM started breaking the existing limits by paving the way for the development of functionalized nanomaterials. A number of theories have been applied in the development of these functionalized nanomaterials. In the invention of carbon nanotubes (CNTs) and other studies of the behaviors of nanostructures, the nonlocal elasticity theory was also applied in the axial vibration analysis of tapered nanorods [1]. The nonlocal continuum mechanics have been applied for nanoplates, nanoshells, and micro/nanoscales of plates [1-35].

Few of the functionalized nanomaterials such as nanographene and nanocarbon fiber, have received attention because of their multifunctionalized character. Graphene and carbon fibers are being use in various sensors in their nano form. The applications of piezoelectric nanofilms (PNFs) and double-piezoelectric-nanofilm (DPNF) systems as nanoelectromechanical sensors for nanoscale mass detection have been studied. The vibration response of the piezoelectric-nanoplate systems is applied in the nanoelectromechanical sensors for the mass detection. The differential equations of motion based on the nonlocal elasticity theory and Hamilton's principle are derived for both PNF-based and DPNF-based nanosensors [21, 22, 24]. In the study of vibration behavior of graphene sheet embedded in elastic medium, the thermo-mechanical vibration analysis has been applied to study the annular and circular graphene sheet, mono-layer graphene sheet, Annular Graphene Sheet Embedded on Visco-Pasternak Foundation, and rectangular graphene sheet embedded in thermal environment [10, 13, 16, 18]. In the modeling and simulation of these materials, differential equations developed and analyzed by both exact and numerical solutions [2, 14, 19].

AM technology which can likewise be termed "layered manufacturing" or "Three-Dimensional (3D) printer or rapid prototyping technology" is a layer-based production process where parts are made layer-by-layer deposition through digitally controlled technique. The new technology has completely changed the Traditional Manufacturing (TM) and qualification paradigm as it provides great opportunities for simultaneous unitization and topological optimization. The 3D printer technology saves materials and weights, lowers the cost of manufacturing of components, facilitates high strength parts production, high efficiency, high quality, and safety, and offers the design flexibility or options in the production of complex shaped parts as well as provides the capacity to make parts without the use of molds. It is a suitable technology for an array of materials, which includes; ceramics, composites, polymers, and metals. Consequently, it has been widely and primarily applied in medical, biomedical engineering, plastics industry, aerospace, and automotive.

Typically, AM processes are generally classified as Friction-Stir Additive Manufacturing (FSAM) and fusion-based and solid-state Additive Manufacturing (AM). The FSAM which is a combination of AM as well as Friction Stir Welding (FSW), is a type of solid-state AM process that involves intense material shear deformation during metal joining process. The schematic diagram of the novel manufacturing process is shown in Fig. 1, arranged plates with one over the other are clamped and a pin stirring tool is implanted into the clamped plates at elevated rotation speed. Although, there is similarity in the non-consumable rotating tool of FSAM and FSW, the stirring pin in FSAM is longer than that of FSW as shown in Fig.1. Moreover, in the FSAM, the length of the pin exceeds the thickness of the plate. From the figure, the non-useable rotating tool is injected into the overlapping metal plates that run along the joint line to facilitate the welding process. The material becomes mildly molten by the generated heat as a result of friction between rotating tool and the workpiece surfaces in contact. The molten material then flows axially and circumferentially around the rotating tool. And as the operation of the stirring tool progresses along the joint line, the material in this path becomes plasticized and develops into a strong bond after cooling and hence yields the needed manufactured material. This process is continued as the plates are introduced and the pin injected until the required shape is achieved.

The possibility and the capability of FSW as an AM technology was proposed by White in his patent in 1999 [36]. Few years later, the FSW technology was utilized as feasible ways for AM. [37]. However, Airbus and Boeing [38, 39] are two companies that have research centers to demonstrate FSAM. The applications of FSAM in aerospace and aviation sectors has also been reported. [40]. Further areas of applications can be found in microstructural enhancement for end product adaptability, graded material manufacturing, fabrication of stiffened structure, and surface composite manufacturing, for aerospace and other engineering industries [40-42]. Through microstructural control, he friction-stir additive manufacturing for high structural performance of an alloy has been examined [43].

The non-beam-based metal friction stir- deposition additive manufacturing has been studied [44] while a state-of art in FSAM has been done recently [45].

Indisputably, the FSAM is a heat transfer process and understanding this process is helpful in the prediction of thermal cycles and evaluation of material thermal properties in thermal applications. Temperature distribution, temperature profile, heating and cooling rates are important factors in thermal analysis of engineering materials. Temperature distribution can be applied in determining the properties temperature-dependent behavior of plates. More so, temperature profile, heating and cooling rates near the material surface can influence its metallurgical microstructure, hardness distribution, thermal cracking and shrinkage, and residual stresses of the material [46]. Thermal related problems can be minimized when the temperature distribution is known. In addition, temperature measurements are difficult to do during the manufacturing process of a moving coordinate system experienced in additive manufacturing because of the production of plastic deformation caused by the translational and rotational motion of the tool. The determination of temperature distribution in a workpiece is also helpful in determining the thermal history of specific locations in the workpiece and thermal profiles at varying times. It is also helpful in determining the thermal history of the metallurgical properties, the thermal stress and the deformation of the workpiece as a result of thermal stress.
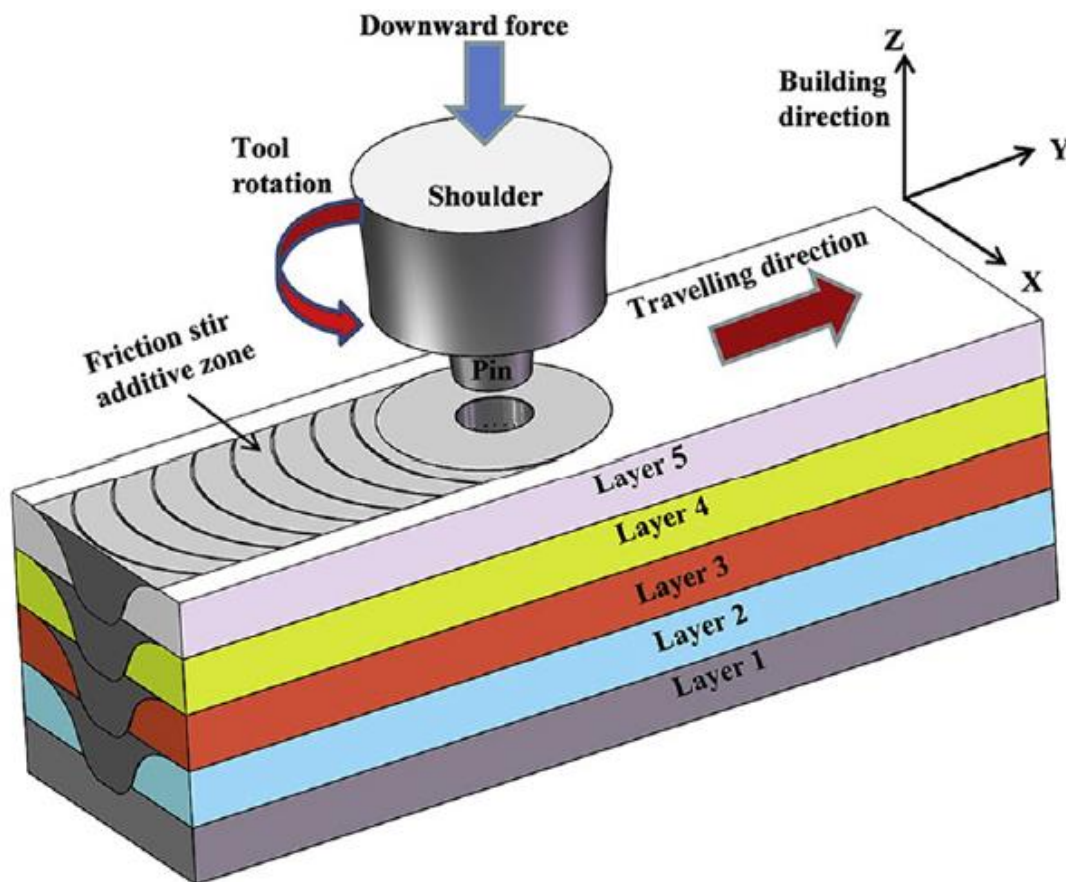
Figure 1. Friction Stir Additive Manufacturing

The effect of temperature on a material heated by moving heat source, at high temperature can result in rapid tool wear, pin thread fracture resulting from thermal shocks, thermal flaking, and inaccurate dimension of workpiece resulting from thermal distortion as well as expansion-contraction behaviors during and after the AM of welding process. Also, the pattern of flow and the variation in temperature during the AM process are critical to engineers for the right design of the processed layout. Hence, it is essential to determine the temperature distribution while carrying out work on the workpiece. Besides, the thermal evaluation of the AM process can be applied for the prediction of the transient temperature behavior, the peak temperature, and the dynamic stress forces and may also be developed to determine the residual stress at the location.

However, in the study of heat flow in metals, little attention has been given to the study of heat flow from moving point source. Few attempts have been made in developing instantaneous point source solution for the exact theory of

moving point heat source in arc welding process [47-49]. In addition, series of studies have been done on increase in temperature near the moving heat source [50]. These studies were however done for only steady-state and linear cases, which make the temperature field appear fixed and unchanging to an observer in motion alongside with the moving heat source. Often times, the solution can be complex for direct real-world applications too [51]. Hence, several experimental and theoretical attempts have been made for real-life description of the temperature profile exhibited by moving heat source. The Fourier series method was applied in the one-dimensional analytical solution of heat conduction from a moving heat source [51]. A simple model for time-dependent line and point sources in welding processes has also been developed [47] and the temperature field of a moving point source with change of state has also been analyzed [52]. In a recent study, the integral transform technique was applied to determine the temperature field resulting from a moving heat source [53]. However, simple analytical solutions can be obtained for the more complicated problems. Therefore, it is very important to first provide simple analytical solutions. This approach leads to better understanding of the problem before attempting the more complex computational methods [47]. For the moving heat source problems, the simple solutions can be applied to develop the more complex solution for heat distributions along the workpiece surface under a steady state heat transfer [47].

Both experimental procedures and mathematical models have been applied to understand the behavior of material during FSAM process. However, the three-dimensional modeling is very much crucial for understanding and detailed analysis of the FSW process. "We lived in a three-dimensional, time-dependent World. The digital computer has enabled the solution of many multi-dimensional problems; however, the solutions of three-dimensional problems are still rare. Inevitably, the analytical solutions of such three-dimensional models are very much more important. Hence, the simple analytical solution for transient three-dimensional temperature distributions for moving heat source problems in the plates during FSAM is presented in this work. The effects of the temperature increase, required time to reach peak temperature, the heating and cooling rates on the distance between the point moving heat source and the centerline were investigated.

2. Problem Formulations

Consider a three-dimensional rectangular coordinate system with a moving heat source during FSAM as shown in Fig. 2. The heat input from the rotating tool pin is simplified as a point moving heat source and it is not dependent of time. The heat generation is at a given rate Q and the heat source moves at a constant velocity *u* along the plate as shown in Fig. 3.
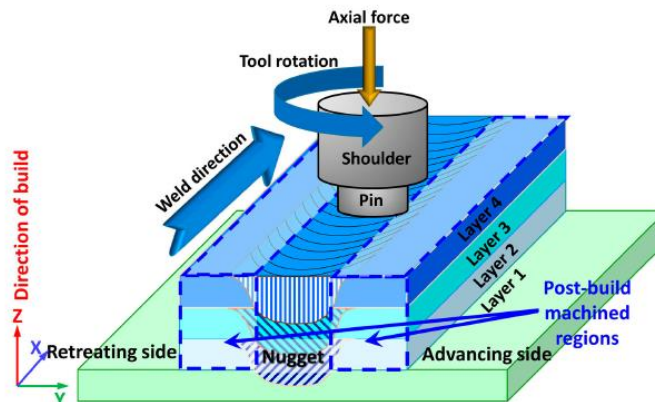
Figure 2. Schematic of multilayer friction stir additive manufacturing process.
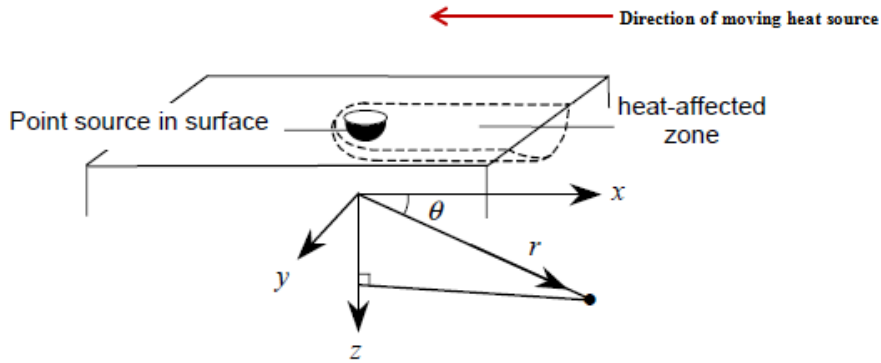
Fig. 3 Point source on the surface of the workpiece [12].

Assuming the workpiece is homogeneous and isotropic, the boundary conditions of the thermal behaviors are symmetrical from the centerline during the manufacturing process, the thermal properties of the workpiece are constant, there is no phase change during the manufacturing process, and the major heat supply is constant and it is from the tool workpiece interface; therefore heat generation at the tool pin/workpiece interface is negligible. Other assumptions include; no heat inflow into and outflow from the workpiece at melting temperature of the material, hence the process is represented by the following governing equation:

$$\frac{\partial T_i}{\partial t} = \alpha \left(\frac{\partial^2 T_i}{\partial x^2} + \frac{\partial^2 T_i}{\partial y^2} + \frac{\partial^2 T_i}{\partial z^2} \right) + \frac{Q_i'''}{k}, \quad i = 1,2,3,4.$$

Where $\alpha = \dfrac{k}{\rho c_p}$, which is the thermal diffusivity and Q_{work} is the heat dissipated at the rate of internal heat generation per unit volume of the workpiece

Initial Conditions

$$t = 0, \quad T_i(x, y, z) = T_o \tag{2}$$

Boundary Conditions

The moving heat source-plate interface has a boundary condition of heat flux given as

$$-k_1 \frac{\partial T_1}{\partial z}\bigg|_{z=0} = \gamma Q_p, \quad in \ the \ range \ R_p \leq r \leq R_s \tag{3}$$

Where R_p and R_s are the radius of the pin and shoulder, respectively. Q_p is the power supplied by the pin and γ is a ratio according to which generated heat at the interface of the tool and workpiece is transferred between both of them and is given as

$$\gamma = \frac{\sqrt{(k\rho c_p)_{plate/workpiece}}}{\sqrt{(k\rho c_p)_{plate/workpiece}} + \sqrt{(k\rho c_p)_{platesource/tool}}}$$

The heat generated at the moving point heat source and workpiece interface $Q_{plate/workpiece}$ is considered to be invariant with *x* and *y*.

The heat exchange boundary conditions between the workpiece top surface and the surrounding is that of convective and radiative conditions

$$-k_1 \frac{\partial T_1}{\partial z}\bigg|_{z=0} = h(T_1 - T_\infty) + \sigma\varepsilon(T_1^4 - T_\infty^4) \tag{4}$$

An effective heat transfer coefficient

$$h_{eff} = h + \sigma \in \left(T^3 + T_\infty T^2 + T_\infty^2 T + T_\infty^3\right) \tag{5}$$

In order to linearize the convective and radiative effects at the boundary conditions given in Eq. (4), thus,

$$-k \frac{\partial T_1}{\partial z}\bigg|_{z=0} = h_{eff}(T_1 - T_\infty), \quad r \geq R_s \tag{6}$$

Interfacial conditions when there is thermal contact resistance between the plates (imperfect thermal contact)

$$-k_1 \frac{\partial T_1}{\partial z}\bigg|_{z=d_1} = h_{eff}(T_1 - T_2), \quad r \geq R_s$$

$$-k_2 \frac{\partial T_2}{\partial z}\bigg|_{z=d_2} = h_{eff}(T_2 - T_3), \quad r \geq R_s \tag{7}$$

$$-k_3 \frac{\partial T_3}{\partial z}\bigg|_{z=d_3} = h_{eff}(T_3 - T_4), \quad r \geq R_s$$

Which can be expressed as

$$-k_i \frac{\partial T_i}{\partial z}\bigg|_{z=d_i} = h_{eff}(T_i - T_{i+1}), \quad r \geq R_s \tag{8}$$

However, if there is perfect thermal contact between the plates

$$T_1\big|_{z=d_1} = T_2\big|_{z=d_1}, \quad -k_1 \frac{\partial T_1}{\partial z}\bigg|_{z=d_1} = -k_2 \frac{\partial T_2}{\partial z}\bigg|_{z=d_1}, \quad r \geq R_s$$

$$T_2\big|_{z=d_2} = T_3\big|_{z=d_2}, \quad -k_2 \frac{\partial T_2}{\partial z}\bigg|_{z=d_2} = -k_3 \frac{\partial T_3}{\partial z}\bigg|_{z=d_2}, \quad r \geq R_s \tag{9}$$

$$T_3\big|_{z=d_3} = T_4\big|_{z=d_4}, \quad -k_3 \frac{\partial T_3}{\partial z}\bigg|_{z=d_3} = -k_4 \frac{\partial T_4}{\partial z}\bigg|_{z=d_4}, \qquad r \geq R_s$$

Which can be expressed as

$$T_i\big|_{z=d_i} = T_{i+1}\big|_{z=d_i}, \quad -k_i \frac{\partial T_i}{\partial z}\bigg|_{z=d_i} = -k_{i+1} \frac{\partial T_{i+1}}{\partial z}\bigg|_{z=d_i}, \qquad r \geq R_s \tag{10}$$

At the bottom surface of the workpiece, heat is lost by conduction and the model for support base is complex. But, in order to overcome the complexity in the models and hence obtain solution to the problem, a high global heat transfer coefficient is assumed and the heat loss is modeled as convective heat flux q_b

$$-k_4 \frac{\partial T_4}{\partial z}\bigg|_{z=d_4} = \beta_b(T_4 - T_\infty) \tag{11}$$

The remaining boundary conditions are taken as ambient temperature

$$\text{i.e.} \quad T\big|_{y=-\infty} = T_\infty \qquad T\big|_{y=\infty} = T_\infty \qquad T\big|_{x=-\infty} = T_\infty \qquad T\big|_{x=\infty} = T_\infty \tag{12}$$

3. Analytical Solution to the Transient State Temperature Distribution Model

In this section, with the aid of Laplace transform, an exact analytical solution is developed for the case when the plates are thermally similar and perfectly in thermal contact. In this case, the energy equations coupled at the interface and temperatures at the interface are equal. The present work is a part of maiden thermal analysis of peak temperatures in FSAM. Therefore, for simplicity and ease of developing exact analytical solutions which are to serve as benchmarks for the numerical/computational analysis of the nonlinear and complex cases, the assumption of constant thermal properties of the workpiece, perfect contact, thermally similar and no phase change are made. Writing the thermal model as

$$\frac{\partial T'}{\partial t} = \alpha \left(\frac{\partial^2 T'}{\partial x^2} + \frac{\partial^2 T'}{\partial y^2} + \frac{\partial^2 T'}{\partial z^2} \right) \tag{13}$$

where $\alpha = \dfrac{k}{\rho c_p}$

Taking $T = T' - T_\infty$ and $r = \sqrt{x^2 + y^2 + z^2}$ as shown in Fig. 3, we arrived

$$\frac{\partial T}{\partial t} = \alpha \frac{\partial^2 T}{\partial r^2} \tag{14}$$

With the initial and boundary conditions are

$$t = 0, \quad 0 \le r \le \infty, \; T = 0$$

$$\hspace{10cm} (15)$$

$$t > 0, \quad r \to \infty, \; T = 0$$

Applying the Laplace transform to Eq. (14), we have

$$\frac{\partial^2 \bar{T}}{\partial r^2} - \frac{s}{\alpha} \bar{T} = 0 \hspace{6cm} (16)$$

The solution of Eq. (16)

$$\bar{T} = A e^{\left(\sqrt{\frac{s}{\alpha}} r \right)} + B e^{\left(-\sqrt{\frac{s}{\alpha}} r \right)} \hspace{4cm} (17)$$

As $t > 0, \quad r \to \infty, \; A = 0$

Therefore,

$$\bar{T} = B e^{\left(-\sqrt{\frac{s}{\alpha}} r \right)} \hspace{6cm} (18)$$

The inverse Laplace transform of Eq.(18) Found as follows

$$T(r,t) = \frac{rB}{2\sqrt{\alpha \pi t^3}} e^{-\left(r^2/4\alpha t \right)} \hspace{4cm} (19)$$

To find B, a small spherical pin of radius a and heat flux Q from the pin surface are considered. There is inflow and outflow of thermal energy across the boundary in and out of the sphere. Hence, the sum of the heat flux across the spherical pin surface is

$$\frac{\dot{q}_p t}{A_c} = \int_{-\infty}^{\infty} \rho c_p T(r,\mathrm{t}) dr$$

$$\frac{\dot{q}_p t}{A_c} = \frac{B \rho c_p}{2\sqrt{\alpha \pi t^3}} \int_{-\infty}^{\infty} r e^{-\left(r^2/4\alpha t \right)} dr$$

$$Since \quad \frac{1}{2\sqrt{\alpha \pi t^3}} \int_{-\infty}^{\infty} r e^{-\left(r^2/4\alpha t \right)} dr = 1, \quad then \; B = \frac{q_p t}{A_c \rho c_p}$$

$\dot{q}_p$ is the power supplied by the pin, r is the radial distance from the point source

Recall $r = \sqrt{x^2 + y^2 + z^2}$

$$T(r,t) = \frac{\dot{q}_p}{2A_c \rho c_p \sqrt{\alpha \pi t}} e^{-\left(r^2/4\alpha t\right)} \tag{20}$$

Recall $r = \sqrt{x^2 + y^2 + z^2}$

$$T(x,y,z,t) = \frac{\dot{q}_p}{2A_c \rho c_p \sqrt{\alpha \pi t}} e^{-\left((x^2+y^2+z^2)/4\alpha t\right)} \tag{21}$$

This is a case where the origin is at (0, 0, 0). For the origin of the co-ordinate system is at (x', y', z'), we have

$$T(x,x',y,z,t) = \frac{\dot{q}_p}{2A_c \rho c_p \sqrt{\alpha \pi t}} e^{-\left([(x-x')^2+(y-y')^2+(z-z')^2]/4\alpha t\right)} \tag{22}$$

However, the motion of the moving heat source at speed "v" is relative to the coordinate system,

$$x' = vt$$

Therefore, the temperature rise is given by

$$T(x,x',y,z,t) = \frac{\dot{q}_p}{2A_c \rho c_p \sqrt{\alpha \pi t}} e^{-\left([(x-vt)^2+y^2+z^2]/4\alpha t\right)} \tag{23}$$

4. Results and Discussion

The developed solution is simulated in MATLAB to graphically show the thermal responses of the plates during the FSAM process as shown in Fig.3. The temperature histories at 8mm form the edge and different depths or plates during the process are shown in Fig. 4 while the temperature variation with respect to time at 2 mm and 8 mm depth from top surface (fourth and first plates) and 8 mm and 16 mm distances from the centerline is shown in Fig. 5.

Fig. 6 shows the temperature variation with respect to time in the material at varying reference point from the centerline. The characteristic features of the temperature profiles such as rapid increase in temperature towards the pin point and slow decrease while withdrawing from the point are shown in the results. The reason for the behavior is that, while the process is ongoing, the heat source encounters cold slab on its path of operation and leaves behind or moves away from hot slab. Furthermore, there is high temperature gradient in the immediate material upfront the tool due to rapid heat transfer, which is unlike the region behind the tool. The temperature profiles of the plates at different plate widths for the four (4) plates is shown in Fig. 8.
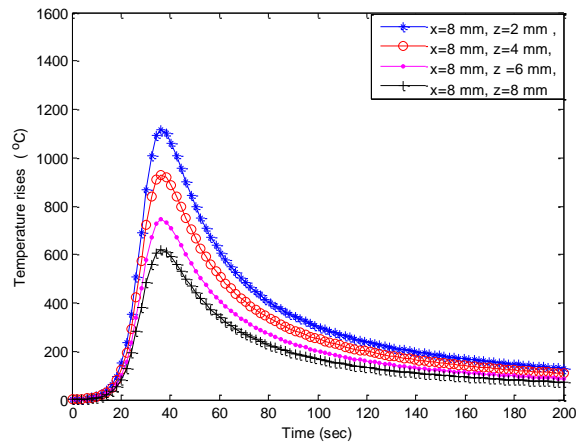
Fig. 4 Temperature profiles for different depths of the material and 8 mm from the centerline.
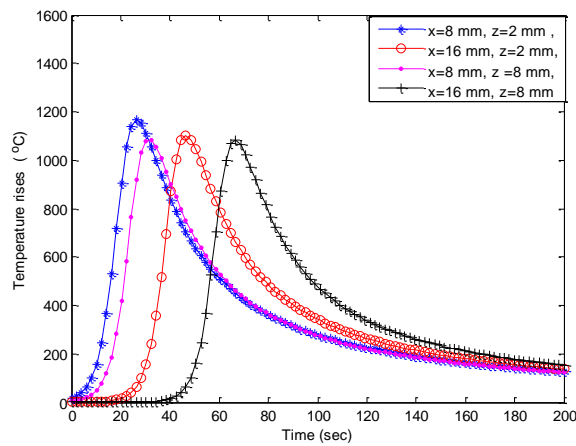
Fig. 5 Temperature profiles for depth 2mm and 8 mm of the material at 8 mm and 16 mm from the centerline.
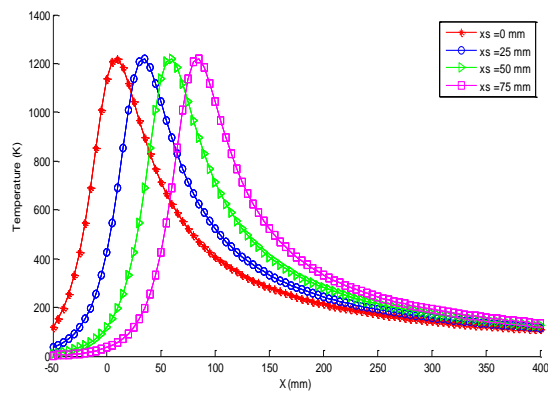
Fig. 6 Temperature profiles in the material at different reference points
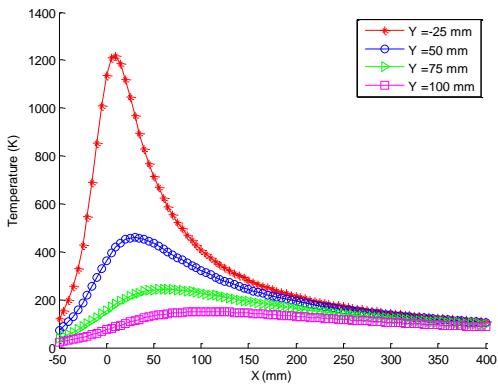
Temperature profiles for different widths in plate 4
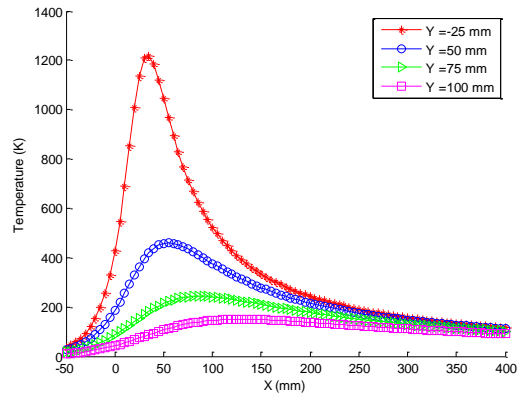
Fig. 7a

Fig. 7b Temperature profiles for different widths in plate 3
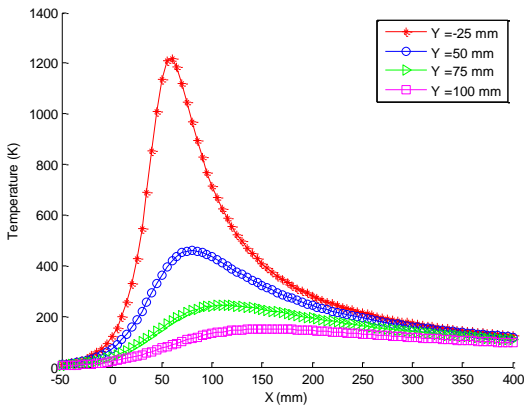
Fig. 7c Temperature profiles for different widths in plate 2
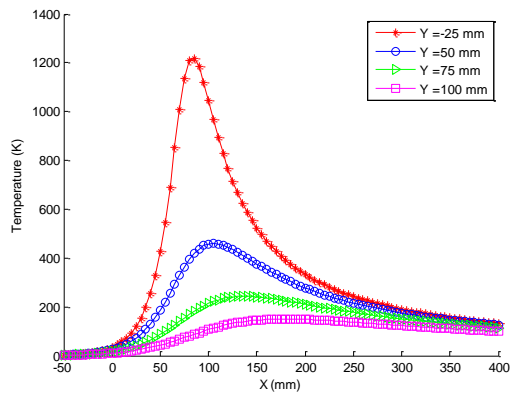
Fig. 7d Temperature profiles for different widths in plate 1
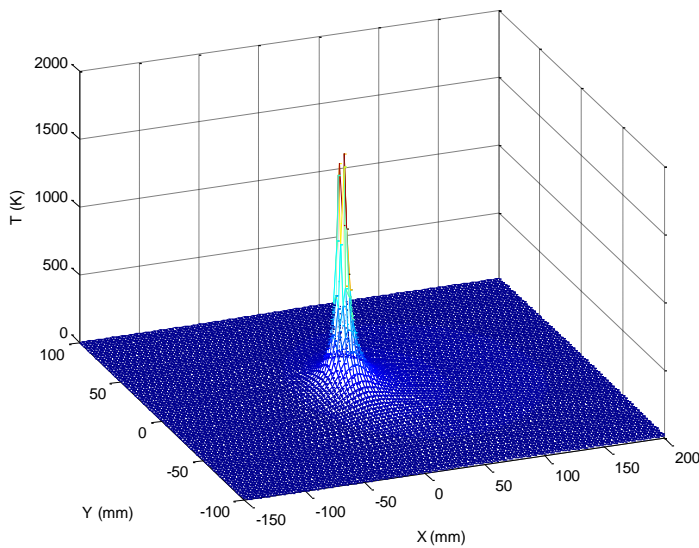
Fig. 8a 3D-plot Temperature increase profiles without pre-heating process in direction when the heat source is at middle of the plates.
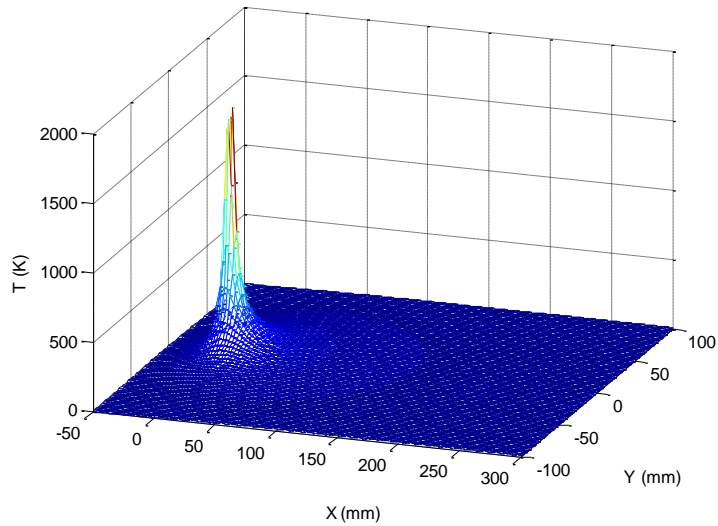
Fig. 8b 3D-plot Temperature increase profiles without pre-heating in direction when the heat source is at 25 mm from the edge of the plates.
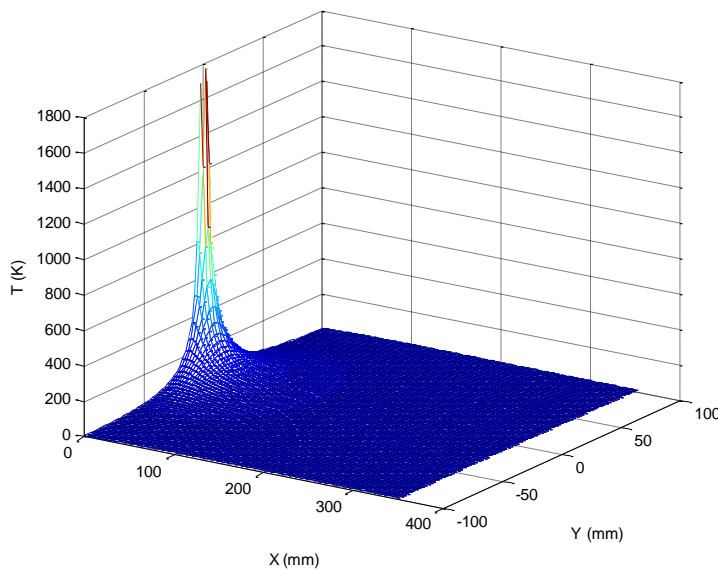
Fig. 9. 3D-plot Temperature increase profiles with pre-heating in process direction when the heat source is at 25 mm from the edge of the plates.

Figs. 8 and 9 show the effect of preheating the peak temperature of the FSAM process. While Figs. 8a and 8b illustrate the three-dimensional plot which shows the maximum temperature in the material without preheating, Fig. 9 shows the effect of preheating on the thermal behaviour of the plates. It is shown that when the plate is preheated, peak temperature in the material increases to $1800^{\mathrm{O}}C$ as against the $1200^{\mathrm{O}}C$ when the material is not preheated. However, the peak temperature depends on the quantity of heat supply for the preheating process. It can be observed that when the initial workpiece temperature is increased, the cooling rate decreases, and this makes the process. The peak temperature also depends on the welding conditions, heat generation the materials, etc. The variation of shoulder heat generation rate with welding rotational speed at different welding velocities of 101, 150 and 200 mm/min depicts that increasing the tool rotational speed at constant weld speed increases the heat input, whereas the heat input decreases with an increase in the weld speed at constant tool rotational speed. It was also established that the fractional heat generation rate is between 80 to 90% heat is generated at the tool shoulder and the remaining

amount at other tool surfaces. However, this depends on the welding conditions. The fraction of heat generated by the probe is estimated to be as high as 20%, which leads to the conclusion that the analytical estimated probe heat generation contribution is not negligible.

Table 1: Comparison of Results

Distance from the center line (mm)	Advanced Side Peak Temperature (ºC)		Retracted Side Peak Temperature (ºC)	
	Experiment	Model	Experiment	Model
11	306.9	298.5	297.5	288.3
15	243.6	232.1	248.3	239.4
17	130.6	121.7	226.3	219.8

To the best of the authors search and knowledge, experimental results on thermal analysis and peak temperature of FSAM were not available as at the time of this present study. However, Table 1 present the comparison of results of the exact analytical solution and experimental study on the peak temperatures of FSW [35]. The results on both, advancing and retreating sides, at 11, 15 and 17 mm from center line of each welded joint developed. These measurements represent the nearest temperature to shear line, which determines stir zone. The results of the experimental and theoretical studies show good agreements.

5. Conclusions
In this study, the analysis of three-dimensional transient thermal behaviours of workpiece processed by FSAM is studied using Laplace transforms method. The peak temperature is approximately 1200ºC but this depends on the welding conditions, heat generation the materials, etc. The variation of shoulder heat generation rate with welding rotational speed at different welding velocities of 100-200 mm/min depicts that increasing the tool rotational speed at constant weld speed increases the heat input, whereas the heat input decreases with an increase in the weld speed at constant tool rotational speed. It was also established that the fractional heat generation rate is between 80 to 90% heat is generated at the tool shoulder and the remaining amount at other tool surfaces. However, this depends on the welding conditions. The obtained results from the simulations for varying observed points show typical features of the temperature profiles and these provide critical analysis of the factors influencing the heat flow models in a moving point heat source. Hence, the developed model and its analytical solution provide the benchmark for obtaining temperature profiles in a point moving heat source during AM process.

Nomenclature
Q Heat source surface area
C_p Heat capacity
Bi Biot number
k Thermal conductivity
v Heat source speed
T Temperature at any arbitrary point
Ta ambient temperature

Greek
α Thermal diffusivity
ρ Density

References

[1]   M. Danesh, A. Farajpour, M. Mohammadi, Axial vibration analysis of a tapered nanorod based on nonlocal elasticity theory and differential quadrature method, *Mechanics Research Communications,* Vol. 39, No. 1, pp. 23-27, 2012.

[2]   H. Mohammadi, M. Ghayour, A. Farajpour, Analysis of free vibration sector plate based on elastic medium by using new version of differential quadrature method, *Journal of Simulation and Analysis of Novel Technologies in Mechanical Engineering,* Vol. 3, No. 2, pp. 47-56, 2010.

[3]   N. GHAYOUR, A. SEDAGHAT, M. MOHAMMADI, WAVE PROPAGATION APPROACH TO FLUID FILLED SUBMERGED VISCO-ELASTIC FINITE CYLINDRICAL SHELLS, *JOURNAL OF AEROSPACE SCIENCE AND TECHNOLOGY (JAST),* Vol. 8, No. 1, pp. -, 2011.

[4]   H. Moosavi, M. Mohammadi, A. Farajpour, S. H. Shahidi, Vibration analysis of nanorings using nonlocal continuum mechanics and shear deformable ring theory, *Physica E: Low-dimensional Systems and Nanostructures,* Vol. 44, No. 1, pp. 135-140, 2011/10/01/, 2011.

[5]   A. Farajpour, M. Danesh, M. Mohammadi, Buckling analysis of variable thickness nanoplates using nonlocal continuum mechanics, *Physica E: Low-dimensional Systems and Nanostructures,* Vol. 44, No. 3, pp. 719-727, 2011.

[6]   A. Farajpour, M. Mohammadi, A. Shahidi, M. Mahzoon, Axisymmetric buckling of the circular graphene sheets with the nonlocal continuum plate model, *Physica E: Low-dimensional Systems and Nanostructures,* Vol. 43, No. 10, pp. 1820-1825, 2011.

[7]   A. G. Arani, S. Maghamikia, M. Mohammadimehr, A. Arefmanesh, Buckling analysis of laminated composite rectangular plates reinforced by SWCNTs using analytical and finite element methods, *Journal of mechanical science and technology,* Vol. 25, No. 3, pp. 809-820, 2011.

[8]   A. Farajpour, A. Shahidi, M. Mohammadi, M. Mahzoon, Buckling of orthotropic micro/nanoscale plates under linearly varying in-plane load via nonlocal continuum mechanics, *Composite Structures,* Vol. 94, No. 5, pp. 1605-1615, 2012.

[9]   M. Mohammadi, M. Goodarzi, M. Ghayour, S. Alivand, Small scale effect on the vibration of orthotropic plates embedded in an elastic medium and under biaxial in-plane pre-load via nonlocal elasticity theory, 2012.

[10]   M. Mohammadi, A. Farajpour, M. Goodarzi, R. Heydarshenas, Levy Type Solution for Nonlocal Thermo-Mechanical Vibration of Orthotropic Mono-Layer Graphene Sheet Embedded in an Elastic Medium, *Journal of Solid Mechanics,* Vol. 5, No. 2, pp. 116-132, 2013.

[11]   M. Mohammadi, M. Goodarzi, M. Ghayour, A. Farajpour, Influence of in-plane pre-load on the vibration frequency of circular graphene sheet via nonlocal continuum theory, *Composites Part B: Engineering,* Vol. 51, pp. 121-129, 2013.

[12]   M. Mohammadi, M. Ghayour, A. Farajpour, Free transverse vibration analysis of circular and annular graphene sheets with various boundary conditions using the nonlocal continuum plate model, *Composites Part B: Engineering,* Vol. 45, No. 1, pp. 32-42, 2013.

[13]   M. Mohammadi, A. Farajpour, M. Goodarzi, H. Mohammadi, Temperature Effect on Vibration Analysis of Annular Graphene Sheet Embedded on Visco-Pasternak Foundation *Journal of Solid Mechanics,* Vol. 5, No. 3, pp. 305-323, 2013.

[14]   M. Mohammadi, A. Farajpour, M. Goodarzi, H. Shehni nezhad pour, Numerical study of the effect of shear in-plane load on the vibration analysis of graphene sheet embedded in an elastic medium, *Computational Materials Science,* Vol. 82, pp. 510-520, 2014/02/01/, 2014.

[15]   A. Farajpour, A. Rastgoo, M. Mohammadi, Surface effects on the mechanical characteristics of microtubule networks in living cells, *Mechanics Research Communications,* Vol. 57, pp. 18-26, 2014/04/01/, 2014.

[16]   M. Mohammadi, A. Farajpour, A. Moradi, M. Ghayour, Shear buckling of orthotropic rectangular graphene sheet embedded in an elastic medium in thermal environment, *Composites Part B: Engineering,* Vol. 56, pp. 629-637, 2014.

[17]   S. R. Asemi, M. Mohammadi, A. Farajpour, A study on the nonlinear stability of orthotropic single-layered graphene sheet based on nonlocal elasticity theory, *Latin American Journal of Solids and Structures,* Vol. 11, No. 9, pp. 1515-1540, 2014.

[18]   M. Mohammadi, A. Farajpour, M. Goodarzi, F. Dinari, Thermo-mechanical vibration analysis of annular and circular graphene sheet embedded in an elastic medium, *Latin American Journal of Solids and Structures,* Vol. 11, pp. 659-682, 2014.

[19]   M. Mohammadi, A. Moradi, M. Ghayour, A. Farajpour, Exact solution for thermo-mechanical vibration of orthotropic mono-layer graphene sheet embedded in an elastic medium, *Latin American Journal of Solids and Structures,* Vol. 11, No. 3, pp. 437-458, 2014.

[20]   M. Goodarzi, M. Mohammadi, A. Farajpour, M. Khooran, Investigation of the effect of pre-stressed on vibration frequency of rectangular nanoplate based on a visco-Pasternak foundation, 2014.

[21]   S. R. Asemi, A. Farajpour, H. R. Asemi, M. Mohammadi, Influence of initial stress on the vibration of double-piezoelectric-nanoplate systems with various boundary conditions using DQM, *Physica E: Low-dimensional Systems and Nanostructures,* Vol. 63, pp. 169-179, 2014.

[22]   S. R. Asemi, A. Farajpour, M. Mohammadi, Nonlinear vibration analysis of piezoelectric nanoelectromechanical resonators based on nonlocal elasticity theory, *Composite Structures,* Vol. 116, pp. 703-712, 2014.

[23]   M. Safarabadi, M. Mohammadi, A. Farajpour, M. Goodarzi, Effect of surface energy on the vibration analysis of rotating nanobeam, 2015.

[24]   H. Asemi, S. Asemi, A. Farajpour, M. Mohammadi, Nanoscale mass detection based on vibrating piezoelectric ultrathin films under thermo-electro-mechanical loads, *Physica E: Low-dimensional Systems and Nanostructures,* Vol. 68, pp. 112-122, 2015.

[25]   M. Goodarzi, M. Mohammadi, M. Khooran, F. Saadi, Thermo-Mechanical Vibration Analysis of FG Circular and Annular Nanoplate Based on the Visco-Pasternak Foundation, *Journal of Solid Mechanics,* Vol. 8, No. 4, pp. 788-805, 2016.

[26]   M. Baghani, M. Mohammadi, A. Farajpour, Dynamic and Stability Analysis of the Rotating Nanobeam in a Nonuniform Magnetic Field Considering the Surface Energy, *International Journal of Applied Mechanics,* Vol. 08, No. 04, pp. 1650048, 2016.

[27]   M. R. Farajpour, A. Rastgoo, A. Farajpour, M. Mohammadi, Vibration of piezoelectric nanofilm-based electromechanical sensors via higher-order non-local strain gradient theory, *Micro & Nano Letters,* Vol. 11, No. 6, pp. 302-307, 2016.

[28]   A. Farajpour, M. Yazdi, A. Rastgoo, M. Mohammadi, A higher-order nonlocal strain gradient plate model for buckling of orthotropic nanoplates in thermal environment, *Acta Mechanica,* Vol. 227, No. 7, pp. 1849-1867, 2016.

[29]   A. Farajpour, M. H. Yazdi, A. Rastgoo, M. Loghmani, M. Mohammadi, Nonlocal nonlinear plate model for large amplitude vibration of magneto-electro-elastic nanoplates, *Composite Structures,* Vol. 140, pp. 323-336, 2016.

[30]   M. Mohammadi, M. Safarabadi, A. Rastgoo, A. Farajpour, Hygro-mechanical vibration analysis of a rotating viscoelastic nanobeam embedded in a visco-Pasternak elastic medium and in a nonlinear thermal environment, *Acta Mechanica,* Vol. 227, No. 8, pp. 2207-2232, 2016.

[31]   A. Farajpour, A. Rastgoo, M. Mohammadi, Vibration, buckling and smart control of microtubules using piezoelectric nanoshells under electric voltage in thermal environment, *Physica B: Condensed Matter,* Vol. 509, pp. 100-114, 2017.

[32]   M. Mohammadi, M. Hosseini, M. Shishesaz, A. Hadi, A. Rastgoo, Primary and secondary resonance analysis of porous functionally graded nanobeam resting on a nonlinear foundation subjected to mechanical and electrical loads, *European Journal of Mechanics - A/Solids,* Vol. 77, pp. 103793, 2019/09/01/, 2019.

[33]   M. Mohammadi, A. Rastgoo, Nonlinear vibration analysis of the viscoelastic composite nanoplate with three directionally imperfect porous FG core, *Structural Engineering and Mechanics, An Int'l Journal,* Vol. 69, No. 2, pp. 131-143, 2019.

[34]   M. Mohammadi, A. Rastgoo, Primary and secondary resonance analysis of FG/lipid nanoplate with considering porosity distribution based on a nonlinear elastic medium, *Mechanics of Advanced Materials and Structures,* Vol. 27, No. 20, pp. 1709-1730, 2020/10/15, 2020.

[35]   M. Mohammadi, A. Farajpour, A. Moradi, M. Hosseini, Vibration analysis of the rotating multilayer piezoelectric Timoshenko nanobeam, *Engineering Analysis with Boundary Elements,* Vol. 145, pp. 117-131, 2022/12/01/, 2022.

[36]   D. White, Object consolidation employing friction joining, *United States Patent,* Vol. 1, pp. https://patents.google, 1999.

[37]   J. J. S. Dilip, G. D. J. Ram, . Additive manufacturing with friction welding and friction deposition processes, *Int J Rapid Manuf,* Vol. 3, pp. 56-69, 2012.

[38]   P. H. Lequeu, R. Muzzolini, J. C. Ehrstro, Power point presentation on: high performance friction stir welded structures using advanced alloys, *WA: Aeromat Conf. Seattle*, 2006.

[39]   J. A. Baumann, Production of energy efficient preform structures *PEEPS*, 2012.

[40]   S. Palanivel, H. Sidhar, R. S. Mishra, Friction stir additive manufacturing: route to high structural performance, *JOM,* Vol. 67, pp. 616–621, 2015.

[41]   R. S. Mishra, Z. Ma, I. Charit, Friction stir processing: a novel technique for fabrication of surface composite, *Mater Sci Eng A,* Vol. 341, pp. 307-310, 2003.

[42]   M. Yuqing, K. Liming, H. Chunping, Formation characteristic, microstructure, and mechanical performances of aluminium-based components by friction stir additive manufacturing, . *Int J Adv Manuf Technol,* Vol. 83, pp. 1637-1647, 2016.

[43]   S. Palanivel, P. Nelaturu, B. Glass, R. S. Mishra, Friction-stir additive manufacturing for high structural performance through microstructural control in an Mg based *WE43 alloy. Mater Des* Vol. 65, pp. 934-952, 2015.

[44]   H. Z. Yu, M. E. Jones, G. W. Brady, R. Y. Griffiths, D. Garcia, H. A. Rauch, Non-beam-based metal additive manufacturing enabled by additive friction stir deposition, *Scr Mater* Vol. 153, pp. 122-130, 2018.

[45]   R. S. Srivastava, S. Maheshwari, A. N. Siddiquee, T. K. Kundra, A review on recent progress in solid state friction-based metal additive manufacturing: friction stir additive techniques, *Rev Solid State Mater Sci* pp. 345-347, 2018.

[46]   Z. B. Hou, R. Komanduri, General Solutions for Stationary/Moving Plane Heat Source Problems in Manufacturing and Tribology, *Int. J. Heat Mass Transfer,* Vol. 43, No. 10, pp. 1679-1698, 2000.

[47]   Z. Hu, Z. Liu, Heat Conduction Simulation of 2D Moving Heat Source Problems Using a Moving Mesh Method, *Advances in Mathematical Physics,* Vol. ID 6067854, pp. 1-16, 2020.

[48]   C. Yang, The determination of two moving heat sources in two-dimensional inverse heat problem, *Applied Mathematical Modelling,* Vol. 30, pp. 278–292, 2006.

[49]   M. Akbari, D. Sinton, M. Bahrami, Moving Heat Sources In A Half Space: Effect Of Source Geometry, *Proceedings of the ASME 2009 Heat Transfer Summer Conferen San Francisco, California,* Vol. HT2009, pp. 1-10, 2009.

[50]   T. Sajid, M. Sagheer, S. Hussain, Impact of Temperature-Dependent Heat Source/Sink and Variable Species Diffusivity on Radiative Reiner–Philippoff Fluid, *Mathematical Problems in Engineering,,* Vol. ID 9701860, pp. 1-16, 2020.

[51]   C. Kim, K, An analytical solution to heat conduction with a moving heat source, *Journal of Mechanical Science and Technology,* Vol. 25, No. 4, 2011.

[52]   Y. Ahire, M, K. P. Ghadle, Determination Of Temperature In Thin Rectangular Plate With Internal Moving Heat Source, *Journal of Applied Science and Computations,* Vol. VI, No. III, 2019.

[53]   Y. Ahire, M, K. P. Ghadle, Three-Dimensional Unsteady State Temperature Distribution of Thin Rectangular Plate with Moving Point Heat Source, *Indian Journal of Materials Science,* Vol. ID 7563215, pp. 1-7, 2016.